One- and Two-dimenisonal Compressive Edge Spectrum Sensing

Carsten Bockelmann, Edgar Beck, Armin Dekorsy

Department of Communications Engineering
University of Bremen
Otto-Hahn-Allee NW1
28359 Bremen
{bockelmann, beck, dekorsy}@ant.uni-bremen.de

Abstract: Future industrial radio systems for Industry 4.0 applications will heavily rely on the management of shared spectrum to provide coexistence of different wireless communication systems and unknown wireless transmitters. A crucial component for successful coexistence management is the estimation of the spectrum of interest to identify active wireless systems and potential interference sources. Monitoring large bandwidths can be very costly in terms of the required bandwidth if classical Shannon-Nyquist signal acquisition is pursued at a sampling rate at least the bandwidth of the signal of interest. For fast and accurate spectrum estimation, we propose a novel approach called Compressive Edge Spectrum Sensing (CES) that allows for a sampling down to 5% of the Nyquist rate without losses in the detection accuracy of occupied and unoccupied spectrum regions.

1 Introduction

Todays wireless industrial communications systems mostly operate in shared spectrum which often leads to spectrum collisions with planned and unplanned wireless activities. In a controlled environment or licensed spectrum planning of spectrum is an important tool to circumvent or at least manage interference between different wireless systems. However, a deterministic management and planning is usually infeasible in shared spectrum. The environment changes dynamically and has to be continuously monitored to enable dynamic management of wireless systems. This coexistence management of wireless systems is required by international norms [iec] and will be an enabler for reliable industrial radio systems of the future. Accurate and fast spectrum estimation is a crucial requirement for coexistence management to first assess the occupation of the available spectrum and second enforce coexistence through management. Therefore, we focus on novel spectrum sensing approaches as an enabler for future wireless systems in shared spectrum.

In the cognitive radio community different approaches to spectrum sensing have been proposed [ALB11]. In principle two approaches are employed in the cognitive radio literature: (i) estimation of the amplitude spectrum or (ii) estimation of the Power Spectrum Density (PSD). Both can be seen as a first step in spectrum estimation for coexistence management, but PSD estimation is one of the most used approaches with very well established estimation methods. Based on the PSD estimate further processing steps are usually required to identify occupied bands, gray spaces or even identify the active systems. These processing steps can vary depending on the targeted metric. Here, we focus on the identification of occupied and free spectrum ranges without any classification. One idea from literature is to identify occupied spectrum bands through edge detection using the first derivative of the PSD inspired by [TG06], which we will take upon and extend in the following. Still, if large bandwidths are to be monitored the required sampling rate is a general challenge in spectrum sensing. Sampling the spectrum at Nyquist rate with sufficient accuracy to identify all active wireless systems of interest drives the cost of sensing hardware up, may lead to higher latencies and is generally wasteful.

Compressive Sensing (CS) [Don06] is a novel approach from signal processing literature to reduce the required sampling rate of arbitrary sampling problems. In Compressive Sensing the structure of the signal to be sampled is exploited to reduce the number of required samples. The main requirement for CS is sparsity in an appropriate basis or dictionary. Fortunately, spectrum estimation can be cast as a sparse estimation problem if the spectrum is not fully used. Thus, the sampling rate can be drastically reduced saving cost in terms of the required hardware. In literature, Compressive Sensing has already been applied to amplitude spectrum estimation [TG07] as well as PSD estimation [CE14] showing promising results. However, in a busy spectrum the PSD may not be very sparse and the remaining spectrum gaps may be quite small reducing the usefulness of the CS approach. Nonetheless, the edges of individual spectra will be detectable in most cases due to well defined spectrum masks. Hence, taking the derivative of the PSD a sparse estimation problem may be obtained again enabling the application of methods from CS.

The main contribution of this paper is the development of edge estimation through Compressive Sensing algorithms. In contrast to literature we use the derivative of the PSD as a basis to achieve a sparse estimation problem instead of first employing classical or CS-based spectrum estimation followed by a separate edge detection step. Furthermore, we show how to extend this edge detection approach to two-dimensional settings and provide simulative as well as practical verification of our approach.

The remainder of the paper is organized as follows: Section 2 introduces the general estimation problem and assumptions, Section 3 outlines the Compressive Edge Spectrum Sensing approach and extensions to two dimensional estimation, Section 4 presents numerical results for one- and two-dimensional Compressive Edge Spectrum Sensing with different parametrization. Then, Software Defined Radio based measurements are described in Section 5. Finally, Section 6 concludes the paper.

2 System Model and Problem Statement

In the following we will first revisit some basics of spectrum estimation in Section 2.1 required to understand the novel contributions in Section 3 and then discuss the practical implications for practical spectrum estimation algorithms in Section 2.2 and the application of CS to the basic model in Section 2.3.

2.1 Basics of Spectrum Estimation

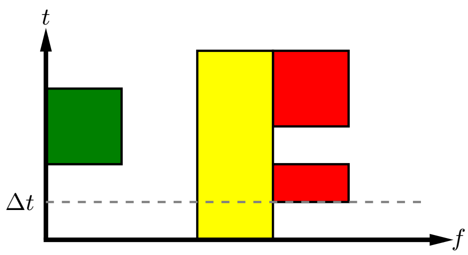

Figure 1: Schematic spectrum occupation in time and frequency. The task of spectrum sensing is to estimate the current spectrum occupation for each time window Δt.

The applications of CS in cognitive radio are manifold [CE14]. However, in this work we introduce the idea of one- and two-dimensional Compressive Edge Sensing (CES). Fig. 1 shows a schematic occupation of spectrum over time. The green, red and yellow areas indicate activity by different systems which need to be sensed. Classically, to estimate the PSD at a given time, the spectrum has to be sampled at Nyquist rate over a time window of length Δt assuming stationarity.

Neglecting noise at the sensing device a complex time-continuous signal $x(t)$ can be observed

$$x(t) = x_1(t) + \ldots + x_U(t)\,, \tag{1}$$

where $x_i(t)\,\forall i = 1, \ldots, U$ are component signals (e.g., red, yellow, green) that are superimposed and define the observed spectrum. By definition the power spectral density $S(f)$ is

$$S(f) = \mathbb{E}\Big\{|C(f)|^2\Big\} = \mathbb{E}\left\{\left|\int_{-\infty}^{\infty} x(t)e^{-j2\pi ft}dt\right|^2\right\} \tag{2}$$

with $C(f)$ denoting the amplitude spectrum and $\mathbb{E}\{\cdot\}$ being the expectation. A common way to estimate the PSD is through the autocorrelation function $r_x(\tau)$

$$S(f) = \int_{-\infty}^{\infty} r_x(\tau) e^{-j2\pi f \tau} d\tau \,, \tag{3}$$

where τ is the time difference in $r_x(\tau) = \mathbb{E}\{x(t)x^*(t-\tau)\}$ and $x^*(t)$ denotes the complex conjugate of $x(t)$. To this point the model is completely continuous. Now, introducing sampling at discrete times $k \cdot T_A$ and T_A being the sample period, the time signal is discretized to $x(k) = x(t = k \cdot T_A)$. Furthermore, we can summarize a number of N samples in a vector $\mathbf{x} \in \mathbb{C}^N$ for convenience. With this discretization the spectrum can be written as

$$\mathbf{s} = \mathbb{E}\Big\{|\mathbf{c}|^2\Big\} = \mathbb{E}\Big\{|\mathbf{F}\mathbf{x}|^2\Big\} \,, \tag{4}$$

where $\mathbf{F}$ is the DFT matrix of size $N \times N$ and the expectation is over the statistics of the discrete samples collected in $\mathbf{x}$. Using $\mathbf{x} = \mathbf{F}^{-1}\mathbf{c}$ the autocorrelation matrix $\mathbf{R}_\mathbf{x}$ summarizing the samples of the autocorrelation function over the N samples then reads

$$\mathbf{R}_\mathbf{x} = \mathbb{E}\big\{\mathbf{F}^{-1}\mathbf{c}\mathbf{c}^H\mathbf{F}^{-H}\big\} = \mathbf{A}\mathbf{R}_\mathbf{c}\mathbf{A}^H = \mathbf{A}\mathrm{diag}\{\mathbf{s}\}\,\mathbf{A}^H \,. \tag{5}$$

with $\mathrm{diag}\{\cdot\}$ forming a matrix with all zeros except for the main diagonal that is equal to the input vector. Furthermore, we define $\mathbf{A} = \mathbf{F}^{-1}$ to ease notation later on. The last equality follows from the autocorrelation matrix of the amplitudes spectrum $\mathbf{c}$ being all-zero except for the main diagonal which is identical to $\mathbf{s}$ due to stationarity. Finally, we can rearrange to

$$\mathbf{r}_\mathbf{x} = \mathrm{vec}\{\mathbf{R}_\mathbf{x}\} = (\mathbf{A}^* \odot \mathbf{A})\,\mathbf{s} = \mathbf{\Phi}\mathbf{s} \tag{6}$$

where $\mathrm{vec}\{\cdot\}$ stacks the columns of a matrix into a long vector and $\odot$ describes the column-wise Kronecker product also termed "Khatri-Rao-Product" leading to $\mathbf{\Phi} \in \mathbb{C}^{N^2 \times N}$. Eq. (6) describes the connection of the discretized PSD $\mathbf{s}$ to the autocorrelation matrix of the discretized signal $\mathbf{x}$. In the next section, we will use this correspondence to introduce novel estimation algorithms based on structural assumptions of $\mathbf{s}$ (sparsity, edges).

2.2 Assumptions and Practical Requirements

Up to this point, we have only considered the theoretical derivations without discussing all the underlying assumptions and implications. Previously, we assumed a stationary statistical signal process that can be observed in an idealized fashion. Furthermore, we assumed that discretization with sampling frequency f_A preserves the spectrum to be estimated and the chosen discretization matches the required fidelity in terms of spectral resolution in the discretized PSD. However, the true estimate of the discretized PSD $\mathbf{s}$ requires infinitely many samples of the signal vector $\mathbf{x}$. Practical estimation of $\mathbf{s}$ usually relies on a finite number of sampled vectors Q collected in time window Δt (cf. Fig. 1) forming a set of vectors $\mathbf{x}_i \in \mathbb{C}^N \, \forall i = 1, \ldots, Q$. Then, averaging over Q vectors the true autocorrelation matrix $\mathbf{R}_\mathbf{x} = \mathbb{E}\{\mathbf{x}\mathbf{x}^H\}$ can be estimated as

$$\mathbf{R}_\mathbf{x} \approx \hat{\mathbf{R}}_\mathbf{x} = \frac{1}{Q}\sum_{i=1}^{Q} \mathbf{x}_i\mathbf{x}_i^H \tag{7}$$

where $\mathbf{x}_i^H$ denotes the hermitian transpose vector.

Furthermore, the number of samples N and the sampling rate $f_A = 1/T_A$ are crucial parameters for accurate spectrum estimation. A common approach is to sample with the Nyquist rate $f_A \geq B$ with B denoting the total bandwidth of the sampled signal $x(t)$. By doing so, it is guaranteed that the discretized signal $\mathbf{x}$ exhibits the same spectrum in the bandwidth of interest as the continuous signal $x(t)$. Still the accuracy of follow-up signal processing steps depends on the frequency resolution of the sampled PSD $\mathbf{s}$ that is determined by the FFT size N given a fixed f_A. As noted above the signal of interest shall be observed in a time window Δt assuming the signal is stationary at least in this window. Then, FFT size N and the time windows length Δt are strictly coupled due to the practical estimation of the autocorrelation through averaging over Q samples, i.e. $\Delta t = QNT_A$. While N determines the frequency resolution with respect to the sampling frequency f_A, the time window Δt is a crucial parameter to balance fast detection and time resolution (small values) against noise suppression (large values).

2.3 Problem Formulation

The Nyquist sampling approach outlined above is a well established method for spectrum estimation. However, if the spectrum exhibits a sparse structure due to low spectrum usage, sampling with or above the Nyquist sampling rate is wasteful. Loosely speaking, the lower the spectrum occupation the sparser the spectrum and hence the lower the occupied bandwidth. If only a fraction of the sensed bandwidth is used the contained information consists of knowing the center frequencies and bandwidths of the few existing sub-spectra. This amounts to a lower information content in the sensed signal and could be interpreted in terms of sparsity. Given the discretized PSD $\mathbf{s}$ most entries s_i will be zero thus leading to a low number of non-zeros. The set of non-zero entries called the support of $\mathbf{s}$ is defined as $\mathcal{S}_{\mathbf{s}} = \{i : s_i \neq 0 \, \forall \, i = 1, \dots, N\}$. The sparsity of $\mathbf{s}$ is then described by the so-called "zero-norm" that counts the non-zeros by the cardinality of the support $\|\mathbf{s}\|_0 = |\mathcal{S}|$.

Compressive Sensing is nowadays a well established new paradigm in signal processing which provides numerous tools and algorithms in the area of sparse signal estimation and detection [Don06]. The main result in CS states that a sparse signal, e.g. the sparse spectrum $\mathbf{s}$, can be estimated from a much lower number of samples M compared to the Nyquist sampling with N samples. Thus, (6) can be modified to sub-Nyquist spectrum estimation by introduction of a sub-sampling or measurement matrix $\mathbf{\Psi} \in \mathbb{C}^{M \times N}$ that describes the linear projection of N Nyquist samples to M Compressive Sensing samples by

$$\mathbf{y} = \mathbf{\Psi x} \tag{8}$$

Now, the same reasoning as above can be applied to spectrum estimation using $\mathbf{y}$ which directly leads to a minor modification of the base equation

$$\mathbf{r_y} = \mathrm{diag}\{\mathbf{R_y}\} = (\mathbf{A}^* \odot \mathbf{A})\, \mathbf{s} = \mathbf{\Phi s} \tag{9}$$

with $\mathbf{A} = \mathbf{\Psi F}^{-1}$ and the overall matrix $\mathbf{\Phi} \in \mathbb{C}^{M^2 \times N}$. Consequently, estimating $\mathbf{s}$ from $\mathbf{y}$ now requires the solution of a differently sized linear equation system, that can only be solved uniquely without further assumptions if $M^2 \geq N$. However, due to the problem structure (9) can only be solved if $M > N/2$ which limits the under-sampling severely. In contrast to this, Compressive Sensing is specifically concerned with cases where $M^2 \ll N$ such that a considerable reduction in sampling rate is achieved by exploiting sparsity. A classical approach to solve (9) for $\mathbf{s}$ is the LASSO operator

$$\hat{\mathbf{s}} = \underset{\mathbf{s} \in \mathbb{C}^N}{\mathrm{argmin}} \|\mathbf{s}\|_1 \quad \text{s.t.} \quad \|\mathbf{r_y} - \mathbf{\Phi s}\|_2 < \epsilon \tag{10}$$

where $\|\cdot\|_1$ and $\|\cdot\|_2$ denote the ℓ_1- and ℓ_2-norm, respectively. Specifically, the ℓ_1-norm induces sparsity in $\mathbf{s}$, whereas the ℓ_2-norm ensures a sensible solution in the squared error sense. Note, that the lasso problem given in (10) has been formulated under the assumption of noise on the samples $\mathbf{y}$ necessitating a squared error formulation with bounded error below ϵ. So far, noise has been neglected to keep the derivations simple. The numerical results presented in Section 4 have been obtained with proper noise assumptions, though.

The PSD $\mathbf{s}$ is only sparse in special cases where the spectrum is usually underused and provides substantial gaps to be used by cognitive radios. In Industry 4.0 scenarios shared spectrum is usually crowded and unused spectrum is much scarer. Hence, assuming $\mathbf{s}$ to be highly sparse is usually unrealistic. Instead, we develop a novel approach called Compressive Edge Spectrum Sensing (CES) in the next section that enables spectrum estimation even in high usage scenarios.

3 Compressive Edge Spectrum Sensing

3.1 One dimensional Edge Spectrum Sensing

With the system model outlined in the previous section, we can now introduce the estimation problem exploiting knowledge beyond the sparsity of the spectrum. Most communication systems adhere to strict spectrum masks which will lead to spectrum edges even in densely occupied spectrum with high probability. Between two spectrally adjacent systems the PSD naturally will have gaps to avoid or minimize interference. These gaps can be exploited as a-priori knowledge in the estimation problem in the form of spectrum edges.

A standard processing step in spectrum estimation for cognitive radios is the detection of edges after PSD estimation [TG06]. The differential of the PSD in terms of the discretized vectors can be achieved through a difference matrix $\mathbf{\Gamma} \in \{-1, 0, 1\}^{N \times N}$ of the form

$$\mathbf{\Gamma} = \begin{pmatrix} 1 & 0 & \cdots & 0 \\ -1 & 1 & \ddots & 0 \\ 0 & \ddots & \ddots & 0 \\ 0 & \cdots & -1 & 1 \end{pmatrix}. \tag{11}$$

In contrast to this two step process of PSD estimation first, and edge detection second, one-dimensional Compressive Edge Sensing estimates the spectrum edges directly. This is achieved by a modification of (9) to introduce the difference matrix $\mathbf{\Gamma}$ applied to the PSD as $\mathbf{z} = \mathbf{\Gamma s}$ yielding

$$\mathbf{r_y} = \mathbf{\Phi \Gamma}^{-1}\mathbf{z} = \tilde{\mathbf{\Phi}}\mathbf{z}\,, \tag{12}$$

where again $\mathbf{r_y}$ denotes the sample autocorrelation of the sub-sampled signal $\mathbf{y}$ and $\mathbf{\Phi}$ denotes the sub-sampling matrix. The spectrum edges are then contained in the sparse vector $\mathbf{z}$. As can be seen from (12), the new sub-sampling matrix $\tilde{\mathbf{\Phi}} \in \mathbb{C}^{M^2 \times N}$ including the difference matrix describes the mapping from edges to observation of the wireless signal completely. Then, reducing the number of samples below Nyquist, i.e., $M \leq \sqrt{N}$, again leads to an under-determined unsolvable equation system. Still, with CS the problem remains solvable due the sparsity of the edge spectrum. Even for $M > \sqrt{N}$ compressive edge detection may provide benefits in terms of noise rejection due to the additional knowledge about the structure of the spectrum that is exploited. The modified edge LASSO then reads

$$\hat{\mathbf{z}} = \underset{\mathbf{z} \in \mathbb{C}^N}{\operatorname{argmin}} \|\mathbf{z}\|_1 \quad \text{s.t.} \quad \|\mathbf{r_y} - \tilde{\mathbf{\Phi}}\mathbf{z}\|_2 < \epsilon \tag{13}$$

Solving (13) yields a sparse estimate $\hat{\mathbf{z}}$ which describes the spectrum edges only. The edges are then the support $\mathcal{S}_{\hat{\mathbf{z}}}$ of $\hat{\mathbf{z}}$. Without further information it is not clear if the spectrum between two adjacent edges given by the vector elements $\hat{z}_i$ and $\hat{z}_j$ with $i, j \in \mathcal{S}$ is occupied or empty. Consequently, a follow up processing step is required that test all adjacent pairs of edges in $\mathcal{S}$. In the following a simple energy detection approach will be employed based on an appropriately chosen noise threshold.

3.2 Two-dimensional Edge Spectrum Sensing

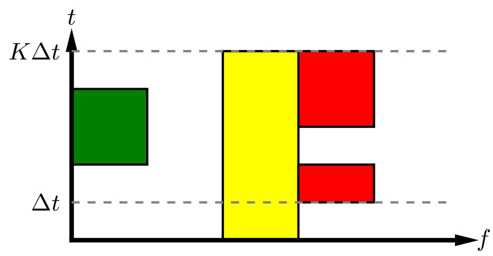

Figure 2: Implications of the two-dimensional approach: a proper time window $K \cdot \Delta t$ is required to estimate edges in time and frequency direction jointly. The basic sampling window Δt still serves to provide noise reduced samples per vector $\mathbf{x}_i\, \forall i = 1, \ldots, K$

The one-dimensional Compressive Edge Sensing outlined in the previous section only exploits edges in the frequency domain resulting from spectrum mask or unoccupied spectrum ranges. However, in the dynamic environment unusually present in industrial scenarios most communication systems are only active for a limited time either to adhere to regulation (duty cycles, short range devices, etc.) or because of intermittent activity (wandering systems, visiting systems). Consequently, the spectrum occupation will change in time and frequency as exemplary depicted in Fig. 2. Such a behavior will result in two-dimensional edges in time and frequency that can be seen as additional structure exploitable by advanced spectrum estimation algorithms. Thus, the two-dimensional Compressive Edge Sensing extends the ideas from the previous section into the time-domain and estimates spectrum as well as time edges. A straightforward approach is to stack K instances of (9) into a single problem of window size $K\Delta t$ yielding

$$\begin{bmatrix} \mathbf{r}_{\mathbf{y}_1} \\ \mathbf{r}_{\mathbf{y}_2} \\ \vdots \\ \mathbf{r}_{\mathbf{y}_K} \end{bmatrix} = \begin{bmatrix} \mathbf{\Phi}_1 & 0 & \cdots & 0 \\ 0 & \mathbf{\Phi}_2 & \cdots & 0 \\ \vdots & \ddots & \ddots & 0 \\ 0 & 0 & \cdots & \mathbf{\Phi}_K \end{bmatrix} \begin{bmatrix} \mathbf{s}_1 \\ \mathbf{s}_2 \\ \vdots \\ \mathbf{s}_K \end{bmatrix} \tag{14}$$

$$\mathbf{r}_T = \mathbf{\Phi}_T \mathbf{s}_T \tag{15}$$

assuming independent realization of the sub-sampling matrices $\mathbf{\Phi}_i \in \mathbb{C}^{M\times N}\,\forall\, i = 1,\ldots,K$.

Similar to the one-dimensional case a difference matrix can now be applied to convert the PSD vector $\mathbf{s}_T$ to form the 2D-edge vector $\mathbf{z}_{\text{2D}} = \mathbf{\Gamma}_{\text{2D}}\mathbf{s}_T$. The definition of the two-dimensional difference matrix is a bit more involved and consist of $\mathbf{\Gamma}_{\text{2D}} = [\mathbf{\Gamma}_f^T \mathbf{\Gamma}_t^T]^T$ with $\mathbf{\Gamma}_f = \mathbf{1}_K \otimes \mathbf{\Gamma}_1$ where $\mathbf{\Gamma}_1 \in \{-1,0,1\}^{N-1\times N}$

$$\mathbf{\Gamma}_1 = \begin{pmatrix} -1 & 1 & 0 & \cdots & 0 \\ 0 & -1 & 1 & \ddots & 0 \\ \vdots & \ddots & \ddots & \ddots & 0 \\ 0 & 0 & \cdots & -1 & 1 \end{pmatrix} \tag{16}$$

and $\mathbf{\Gamma}_t \in \{-1,0,1\}^{(K-1)N\times KN}$

$$\mathbf{\Gamma}_t = \begin{pmatrix} -1_{1,1} & 0 & \cdots & 1_{1,N+1} & 0 & \cdots & 0 & \\ 0 & -1_{2,2,} & \cdots & 0 & 1_{2,N+2} & \cdots & 0 & \\ \vdots & \vdots & \ddots & \vdots & \vdots & \ddots & \vdots & \\ 0 & 0 & \cdots & -1_{(K-1)N,(K-1)N} & 0 & 0 & \cdots & 1_{(K-1)N,KN} \end{pmatrix}. \tag{17}$$

Introducing the two-dimensional differential on the resulting PSD then leads to an equivalent equation system as in (12), which can be solved by an equivalent LASSO problem

$$\hat{\mathbf{s}}_T = \underset{\mathbf{s}_T\in\mathbb{C}^{KN}}{\operatorname{argmin}} \|\mathbf{\Gamma}_{\text{2D}}\mathbf{s}_T\|_1 \quad \text{s.t.} \quad \|\mathbf{r}_T - \mathbf{\Phi}_T\mathbf{s}_T\|_2 < \epsilon \tag{18}$$

that effectively solves the Total Variation (TV) norm by application of the 2D difference matrix. The resulting time-frequency edge spectrum principally leads to even sparser $\mathbf{z}_{\text{2D}}$ and potentially enables stronger sub-sampling. However, due to the processing of K time-windows in one pass the processing delay is increased accordingly.

4 Simulative Evaluation

For the simulative evaluation we assume a test setup in the 2.4 GHz ISM band with WLAN systems of 20 MHz bandwidth placed in a total sensed bandwidth of 100 MHz. The WLAN spectra are modeled as random Gaussian and the spectrum occupation is chosen to follow a simple on-off Markov-Model with two active bands on average, i.e., $\beta = 40\%$ of the sensed spectrum are occupied on average. All Signals and the measurement noise are generated such that the carrier to noise ratio (CNR) randomly lies between 16 dB and 21 dB. The channel is idealized and modeled as pure AWGN without Rayleigh fading or Shadowing effects.

Given the test setup sensing parameters are chosen as follows:

- All $\mathbf{\Psi}_i$ are assumed equal $\mathbf{\Psi}_1 = \mathbf{\Psi}_2 = \ldots = \mathbf{\Psi}_K$
- Elements of $\mathbf{\Psi}$ are random Gaussian distributed with $\mathcal{N}_C(0, 1/N)$
- FFT resolution $N = 100$
- Autocorrelation averaging $Q = 1000$

- Time window of $K = 50$ for two-dimensional CES
- Orthogonal Matching Pursuit (OMP) as the CS solver
- Energy detection with noise based threshold to decide for band occupation

4.1 Results of one- and two-dimensional CES

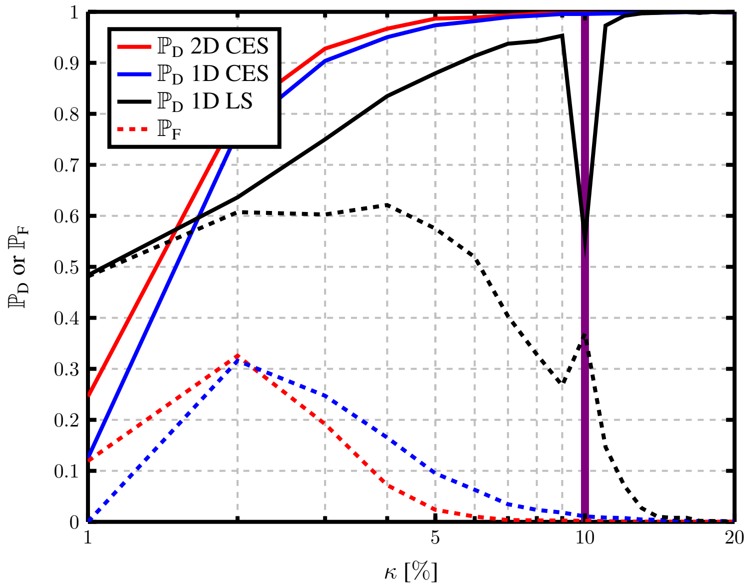

Figure 3: Detection (solid) and false alarm (dashed) rate of 1D and 2D Compressive Edge Sensing over compression κ in percent of the Nyquist sample rate assuming $Q = 1000$, $N = 100$ and $K = 50$ for 2D CES.

The main result is shown in Fig. 3 depicting the achieved detection $\mathbb{P}_D$ (solid) and false alarm $\mathbb{P}_F$ (dashed) rates of 1D and 2D Compressive Edge Sensing (CES). The CS based algorithms are compared to a standard least squares (LS) solution. Due to the dimensions of the equation system that is used to estimate the edge spectrum even the LS approach can reduce the number of samples down to 20% of the Nyquist samples without severe effects on the detection rates. At $\kappa = 10\%$ the least square solution faces numerical problems due to $M = \sqrt{N}$ that can be alleviated by regularization. Below $\kappa = 20\%$ the detection rate slowly declines towards 50%. This behavior could be interpreted as robustness against sub-sampling. However, observing that the false alarm rate also raises to 50% this actually means that the LS solution deteriorates to a random decision on activity after a certain point. The 1D and 2D Compressive Edge Sensing results depicted in blue and red show a different behavior. First, the sampling rate can be reduced down to 10% and even to 5% of the Nyquist rate while detection performance is still near perfect with only a slight penalty in false alarms. Second, below $\kappa = 5\%$ the detection rate quickly falls towards zero while the false alarm rate also tends to zero. Hence, the spectra are not randomly detected as active or inactive but the whole solution tends to zero output. Overall, the 1D and 2D sensing degrade in a graceful fashion meaning that lower κ or in turn higher occupations β do not lead to sudden failures.

The presented results are only one parametrization chosen to perform well in this context. In the following we shortly discuss the influence of Q and N on the performance to point out performance-complexity trade-offs. In the interest of brevity we will focus on one-dimensional CES; the outlined observations are equally valid for two-dimensional CES.

4.2 Parametrization

Fig. 4 shows the detection and false alarm rates for one-dimensional CES in dependence of the number of averaged sample vectors Q, the parametrization of $Q = 1000$ chosen in the setup presented before is indicated

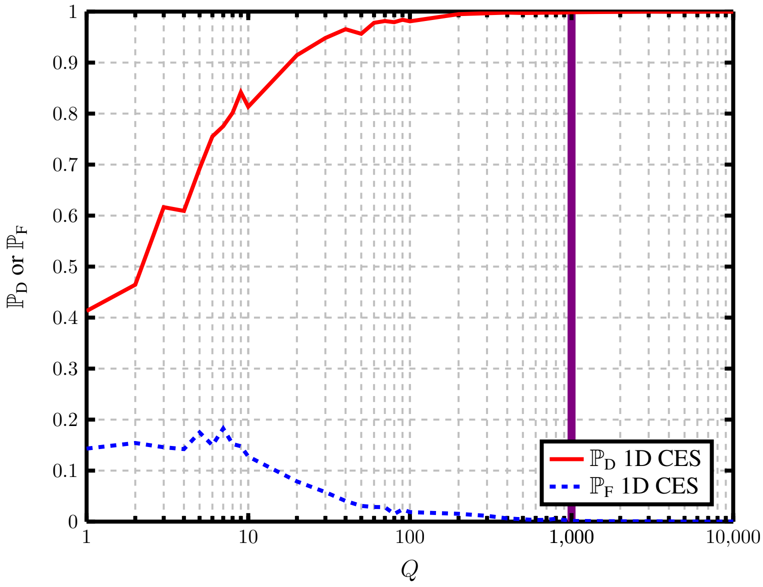

Figure 4: Detection (solid) and false alarm (dashed) rate of 1D CES dependent on the number of averaged sample vectors Q with $\kappa = 15\%$.

by the purple vertical line. From the figure we can immediately see that below $Q = 100$ the detection performance decreases with smaller Q while the false alarm rate $\mathbb{P}_\mathrm{F}$ begins to increase. The main reason for this behavior lies in the decreased quality of the autocorrelation estimate. Eq. (7) is a biased estimator of the true autocorrelation with variance going to zero for Q going to infinity. Consequently, above $Q = 100$ the detection and false alarm rates are improved with diminishing returns at the cost of longer averaging times and hence a reduced time resolution. The working point $Q = 1000$ provides a reasonable trade-off between performance and averaging time but could be lowered in practical applications with mild losses.

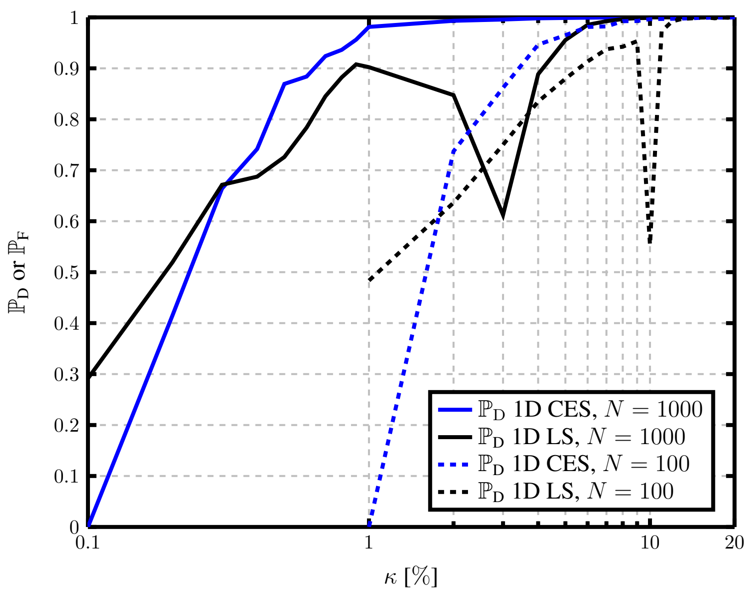

Figure 5: Detection rates for 1D CES (solid) and LS (dashed) for two different N, $Q = 1000$, $\kappa = 15\%$.

In contrast to the averaging parameter Q the FFT size N has a direct impact on the frequency resolution. The larger N, the finer the frequency grid which allows for a higher detection precision of the occupied bands. Furthermore, the detection model (9) scales with N increasing the number of unknowns in $\mathbf{z}$ as well as the matrix size of $\mathbf{\Phi}$. The larger equation system increases complexity accordingly. Due to the fact that the number of edges in $\mathbf{z}$ does not change with N, the relative sparsity normalized to N increases. In CS theory, this leads to an increased detection performance which can be observed in Fig. 5. The figure depicts the performance of 1D CES and the LS approach for two different choices of $N = 100$ and $N = 1000$. Here, the x-axis is scaled differently compared to other figures. For $N = 1000$ a range of $\kappa \in [0.1, 20]$ has been simulated due to the increased performance whereas for $N = 100$ the standard range $\kappa \in [1, 20]$ is used. Clearly, $N = 1000$ enables superior detection performance with a much larger reduction in the sampling rate. However, comparable performance to the $\kappa = 10\%$ for $N = 100$ is achieved at $\kappa \approx 3\%$ for $N = 1000$. Thus, in terms of the absolute number of samples we overall need three times more samples for the same quality level at $N = 1000$. Note, that this is just true in the chosen scenario with WLAN systems of 20 MHz bandwidth. With lower system bandwidths, e.g. Bluetooth, performance differences may be in favor of the higher resolution offered with $N = 1000$. Again, the achieved performance gain will diminish with increasing N approaching the asymptotic performance of the CS detection problem. Finally, it is obvious that the LS solution also performs better with larger N due to $M > N/2$.

5 Practical Verification

In the previous section all results have been obtained via pure simulation following the general assumptions outlined above. However, for practical verification we also build a test setup consisting of two Lyrtech/Nutaq Software Defined Radios (SDR) with 4 phase-coupled MAX2829-Single-Chip RF transceivers working in the 2.4 GHz and 5 GHz Bands. The RF chains offer up to 40 MHz of bandwidth and both SDRs are equipped with eight 12 bit DACs and eight 14bit ADCs with up to $f_A = 105$ MHz sampling rate.

A simple Line Of Sight (LOS) sensing scenario has been defined as follows: Due to limitations in memory bandwidth only a reduced sampling rate of $f_A = 26$ MHz can be realized. In contrast to the simulations that use an overall bandwidth of 100 MHz, here we scaled the test spectra accordingly. The TX-SDR randomly generates Gaussian-distributed signals at different center frequencies to model the WLAN spectra scaled to a maximum bandwidth of 5.2 MHz. All four transceiver chains are used to transmit the generated spectra such that different spectra experience different channel conditions. At approximately 8m distance the RX-SDR uses a single transceiver chain to sense the spectrum and reconstruct the emitted test spectra using offline processing in Matlab. Both the transmit power level as well as the receive amplification have been adjusted to exploit the full dynamic range of the 14 bit ADCs at the receiver.

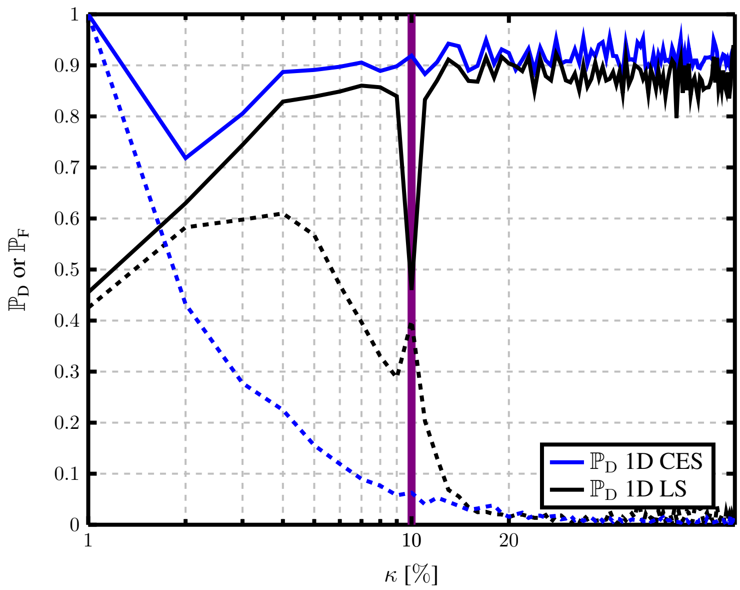

Figure 6: Detection (solid) and false alarm (dashed) rate of 1D and 2D Compressive Edge Sensing over compression in percent of the Nyquist sample rate. Practical Verification with Lyrtech SDR: test spectra scaled to 26 MHz total sensing bandwidth were transmitted line of sight to a sensing unit sampling at Nyquist rate. Sub-sampling and processing are performed via offline processing in Matlab.

Fig. 6 depicts the detection as well as the false alarm rate achieved by offline spectrum estimation using one-dimensional CES and LS according to the setup outlined above. In comparison to the simulated performance results a constant offset in the detection rate is obvious. Hence, the maximum detection performance in this verification scenario lies around 90% detection rate ignoring the outliers at $\kappa = 1\%$. This offset is caused by multi-path propagation in the lab environment that was not considered in the simulations presented before. Due to effects of fast fading spectrum edges might disappear in fading holes or fading might introduce a gap in the middle of an occupied band creating new edges. Thus, the overall performance is decreased which can only be compensated by channel estimation or diversity, e.g. MIMO approaches or cooperative sensing.

Comparing Fig. 3 and Fig. 6 directly and adjusting for the performance offset, the simulated performance still matches the performance of the test setup very well. Minor differences are visible at very low and very high κ but the performance region of interest around $\kappa = 10\%$ shows comparable detection and false alarm rates. As a first verdict, the presented Compressive Edge Spectrum Sensing methods show robust performance in practical scenarios and may be a candidate for fast spectrum estimation in dynamic coexistence management.

Obviously, the SDR hardware is of high quality with low distortion, I/Q imbalances and low CFO variations. Furthermore, we optimized the setup to exploit the full dynamic range of the ADCs. Future investigations should consider the effect of hardware imperfections of lower end transceiver chains and dynamic range mismatches to characterize the effects on detection quality.

6 Conclusion

In this paper we have presented a novel approach to spectrum sensing for cognitive radio and coexistence problems. Based on ideas from Compressive Sensing the spectrum to be estimated can be cast as a sparse estimation problem in the one- or two-dimensional edge description. Using CS reconstruction algorithms spectrum edges can then be found with high accuracy and reliability. The presented results show a reduction in sampling rate to 5% of the Nyquist sampling rate in selected scenarios which is a tremendous complexity reduction on the Analog-to-Digital conversion. Also, the practical verification of the approach using an SDR to sense WLAN test spectra demonstrates the principal feasibility even with standard sampling hardware. In this case just the amount of sampled data is reduced which can be used to lessen the communication load in a network of connected sensing devices. As a first verdict, the presented Compressive Edge Spectrum Sensing methods show robust performance in practical scenarios and may be a candidate for fast spectrum estimation in dynamic coexistence management. However, further investigations are required to develop the CES concept towards a practical and hardware adapted spectrum estimation tool.

References

[ALB11] I.F. Akyildiz, B.F. Lo, and R. Balakrishnan. Cooperative Spectrum Sensing in Cognitive Radio Networks: A Survey. *Physical Communication*, 4(1), March 2011.

[CE14] D. Cohen and Y.C. Eldar. Sub-Nyquist Sampling for Power Spectrum Sensing in Cognitive Radios: A Unified Approach. *IEEE Transactions on Signal Processing*, 62(15), August 2014.

[Don06] D.L. Donoho. Compressed Sensing. *IEEE Transactions on Information Theory*, 52(4):1289–1306, April 2006.

[iec] IEC 62657-2: Industrial communication networks- Wireless communication networks- Part 2: Coexistence management. Technical report.

[TG06] Z. Tian and G.B. Giannakis. A Wavelet Approach to Wideband Spectrum Sensing for Cognitive Radios, 2006.

[TG07] Z. Tian and G.B. Giannakis. Compressed Sensing for Wideband Cognitive Radios. In *IEEE International Conference on Acoustics, Speech and Signal Processing (ICASSP)*, pages 1357–1360, August 2007.